Relationship between ROS production, MnSOD activation and periods of fasting and re-feeding in freshwater shrimp *Neocaridina davidi* (Crustacea, Malacostraca)

Agnieszka Włodarczyk [1], **Grażyna Wilczek** [2], **Piotr Wilczek** [3], **Sebastian Student** [4], **Anna Ostróżka** [1], **Monika Tarnawska** [2], **Magdalena Rost-Roszkowska** [Corresp. 1]

[1] Department of Animal Histology and Embryology, University of Silesia in Katowice, Katowice, Poland

[2] Department of Animal Physiology and Ecotoxicology, University of Silesia in Katowice, Katowice, Poland

[3] Bioengineering Laboratory, Heart Prosthesis Institute, Zabrze, Poland

[4] Faculty of Automatic Control, Silesian University of Technology, Gliwice, Poland

Corresponding Author: Magdalena Rost-Roszkowska
Email address: magdalena.rost-roszkowska@us.edu.pl

The middle region of the digestive system, the midgut of freshwater shrimp *Neocaridina davidi* is composed of a tube-shaped intestine and the hepatopancreas formed by numerous caeca. Two types of cells have been distinguished in the intestine, the digestive cells (D-cells) and regenerative cells (R-cells). The hepatopancreatic tubules have three distinct zones distinguished along the length of each tubule – the distal zone with R-cells, the medial zone with differentiating cells, and the proximal zone with F-cells (fibrillar cells) and B-cells (storage cells). Fasting causes activation of cell death, a reduction in the amount of reserve material, and changes in the mitochondrial membrane potential. However, here we present how the concentration of ROS changes according to different periods of fasting and whether re-feeding causes their decrease. In addition, the activation/deactivation of mitochondrial superoxide dismutase (MnSOD) was analyzed. The freshwater shrimps *Neocaridina davidi* (Crustacea, Malacostraca, Decapoda) were divided into experimental groups: animals starved for 14 days, animals re-fed for 4, 7, and 14 days. The material was examined using the confocal microscope and the flow cytometry. Our studies have shown that long-term starvation increases the concentration of free radicals and MnSOD concentration in the intestine and hepatopancreas, while return to feeding causes their decrease in both organs examined. Therefore, we concluded that a distinct relationship between MnSOD concentration, ROS activation, cell death activation and changes in the mitochondrial membrane potential occurred.

Relationship between ROS production, MnSOD activation and periods of fasting and re-feeding in freshwater shrimp *Neocaridina davidi* (Crustacea, Malacostraca)

Włodarczyk A.[1], Wilczek G. [2], Wilczek P. [3], Student S.[4], Ostróżka A.[1], Tarnawska M.[2], Rost-Roszkowska M.[1*]

[1] University of Silesia in Katowice, Department of Animal Histology and Embryology, Katowice, Poland

[2] University of Silesia in Katowice, Department of Animal Physiology and Ecotoxicology, Katowice, Poland

[3] Heart Prosthesis Institute, Bioengineering Laboratory, Zabrze, Poland

[4]Faculty of Automatic Control, Electronics and Computer Science, Silesian University of Technology, Gliwice, Poland

Corresponding Author

Magdalena Rost-Roszkowska,

Department of Animal Histology and Embryology, University of Silesia in Katowice, Bankowa 9, 40-007 Katowice

email: magdalena.rost-roszkowska@us.edu.pl

23

Abstract

The middle region of the digestive system, the midgut of freshwater shrimp *Neocaridina davidi* is composed of a tube-shaped intestine and the hepatopancreas formed by numerous caeca. Two types of cells have been distinguished in the intestine, the digestive cells (D-cells) and regenerative cells (R-cells). The hepatopancreatic tubules have three distinct zones distinguished along the length of each tubule – the distal zone with R-cells, the medial zone with differentiating cells, and the proximal zone with F-cells (fibrillar cells) and B-cells (storage cells). Fasting causes activation of cell death, a reduction in the amount of reserve material, and changes in the mitochondrial membrane potential. However, here we present how the concentration of ROS changes according to different periods of fasting and whether re-feeding causes their decrease. In addition, the activation/deactivation of mitochondrial superoxide dismutase (MnSOD) was analyzed. The freshwater shrimps *Neocaridina davidi* (Crustacea, Malacostraca, Decapoda) were divided into experimental groups: animals starved for 14 days, animals re-fed for 4, 7, and 14 days. The material was examined using the confocal microscope and the flow cytometry. Our studies have shown that long-term starvation increases the concentration of free radicals and MnSOD concentration in the intestine and hepatopancreas, while return to feeding causes their decrease in both organs examined. Therefore, we concluded that a distinct relationship between MnSOD concentration, ROS activation, cell death activation and changes in the mitochondrial membrane potential occurred.

Key words: digestive system, midgut, epithelium, starvation, free radicals

Introduction

An animal organ which is exposed to various stressors originating from the environment is the midgut (the middle region of the digestive system). It takes part in maintenance of homeostasis of the entire organism. In nature, organisms can be exposed to periodic lack of food or various external harmful stressors, and as a result have evolved mechanisms that help animals to survive in adverse environmental conditions. The midgut is the main place of accumulation of reserve material in invertebrates, which may be used during starvation (*Cervellione et al., 2017*). Therefore the processes related to the survival strategy during exposure to starvation are observed primarily in this organ. Long-term periods of starvation can cause numerous changes at the physiological, biochemical and molecular levels which lead to increased ability to survive (*Wilczek et al., 2014; Lipovšek et al., 2015, 2018; Lipovšek and Novak, 2015; Włodarczyk et al., 2017, 2019*). Starvation can affect and damage many organelles, including the mitochondria (*Ratcliffe and King, 1969; Włodarczyk et al., 2017*), which are responsible for e.g. synthesis of ATP and reactive oxygen species (ROS), or activation of cell death (*Martin, 2010; Kamogashira et al., 2015; Włodarczyk et al., 2019*). Ultrastructural alterations of mitochondria (*Fernandez-Checa, 2003; Faron et al., 2015; Włodarczyk et al., 2017*) also cause changes in the functioning of the enzyme system. In several places along the mitochondrial respiratory chain (mainly due to complexes I and III), electrons can react directly with oxygen or another electron acceptor and generate free radicals. As a result, the superoxide anion radical (O_2-), hydroxide ions (OH^-), and hydrogen peroxide (H_2O_2) are formed. They must be eliminated by activation of the precise enzymatic system (*Cadenas and Davies, 2000; Ramalho-Santos et al., 2009; Yao et al. 2004, 2007; Hung et al., 2014*). Among the antioxidant enzymes, the superoxide dismutases (SOD) play protective roles against the effect of free radicals on organelles, e.g. mitochondria (*Zelko et*

al., 2002; Zhang et al. 2007; Combelles et al., 2009; Umasuthan et al. 2012; Faron et al., 2015). Based on associated metal cofactors, four classes of SOD have been distinguished: Cu/ZnSOD, MnSOD, FeSOD and NiSOD (*Fridovich, 1995; Zelko et al., 2002*). However, the Cu/ZnSOD commonly present in vertebrates has been replaced by MnSOD in crustaceans that is connected with the transport of oxygen by copper from haemocyanin (*Brouwer et al., 2003*). Two types of this enzyme can be recognized: cytMnSOD and mtMnSOD. mtMnSOD has been described as commonly distributed in animals, plants and bacteria, while cytMnSOD has been found only in Crustacea such as prawns, crabs, lobsters, and shrimps (*Brouwer et al., 2003; Lin et al. 2010; Gomez-Anduro et al., 2012*).

The digestive system of malacostracan Crustacea is composed of the tube-shaped ectodermal fore- and hindgut, while the endodermal midgut can be differentiated into intestine and hepatopancreas (*Herrera-Alvarez et al., 2000; Sousa and Petriella, 2006; Sonakowska et al., 2015; Sacristán et al., 2014, 2016; Cervellione et al., 2017*). Many studies have been conducted on crustaceans that have been starved, but they mainly concern the physiological alterations in organisms and they were conducted on species that are adapted to short-term periods of starvation, connected with e.g. molting or to long-term starvation (*Sacristán et al., 2016)*. However, our previous studies on freshwater shrimp *Neocaridina davidi* (formerly *Neocaridina heteropoda*) were focused on long-term starvation. This species originates from Taiwan and it gained its popularity thanks to ease of breeding. In addition, its natural environment and feeding habitats resemble those observed in the majority of freshwater crustaceans all over the world. The midgut of *N. davidi* is composed of a tube-shaped intestine and the hepatopancreas formed by numerous caeca (*Sonakowska et al., 2015*). Two types of cells have been distinguished in the intestine, the digestive cells (D-cells) and regenerative cells (R-cells), while the structure of the

hepatopancreas is more complicated. It is formed by numerous tubules with three distinct zones distinguished along the length of each tubule – the distal zone with R-cells, the medial zone with differentiating cells, and the proximal zone with F-cells (fibrillar cells) and B-cells (storage cells) (*Sonakowska et al., 2015, 2016*). The impact of fasting and re-feeding on ultrastructural changes and activation of cell death in the midgut epithelium of this species has also been described (*Włodarczyk et al., 2017, 2019*). Fasting causes activation of cell death, a reduction in the amount of reserve material, and changes in the mitochondrial membrane potential. These alterations are probably the mechanisms which enable an animal to survive. However, re-feeding reverses all these changes (*Włodarczyk et al., 2017, 2019*). In order to gain a full view of the described changes, we decided to investigate how the concentration of ROS changes according to different periods of fasting and, what is the most important, whether re-feeding causes their decrease. In addition, the activation/deactivation of one of the stress-responsive factor important in antioxidative processes – mitochondrial superoxide dismutase (MnSOD) – was analyzed.

Material & Methods

Materials

The research was conducted on adult specimens of the freshwater shrimp *Neocaridina davidi* (formerly named as *N. heteropoda*) (Crustacea, Malacostraca, Decapoda). The specimens were obtained from local shrimp breeders and kept in a laboratory breeding facility, i.e. a 40 L shrimp tank equipped with heater with thermostat and mechanical filtration system. The water temperature was set to 21 °C, pH to 7 and total water hardness was 10 °d. The *N. davidi* shrimps were fed with JBL Novo Prawn. For the experiment, adult shrimps with cephalothorax length

over 2.5 mm were chosen. The specimens were in good condition, actively moving and taking in food. To collect the material no specific permissions were required for locations/activities.

Experiment. The fasting experiment was performed by placing shrimps in isolated plastic (250 mL) containers. Every day 10% of the water amount was replaced and the plastic containers were cleaned of excrements. Containers were kept in a shaded room to avoid development of algae. Shrimps were starved for 14 days. Specimens were collected for studies. Additionally, some specimens from the experimental group were re-fed for 4, 7, and 14 days. The periods of starvation and re-feeding were established according to our previous experiments and the results obtained (*Włodarczyk et al., 2017, 2019*). The number of specimens from the experimental group that were collected for the experiment and all techniques used are presented in Table 1. Individuals of *N. davidi* were slightly anesthetized on ice and midguts were dissected.

Methods

Confocal microscopy

Dihydroethidium (DHE) – a dye commonly used to evaluate reactive oxygen species (ROS) production, which penetrates all cell membranes. Isolated organs, without fixation, were washed in PBS (phosphate-buffered saline) with 0.0025% Triton X100 (RT) and stained with 30 μM DHE (Invitrogen) prepared from the 30 mM stock solution of DHE in DMSO. Tissues were incubated with the dye for 15 minutes in a dark chamber, at room temperature. After washing the material with PBS, it was labeled with DAPI (30 min in darkness). The material was analyzed with an Olympus FluoView FV1000 confocal microscope.

Superoxide dismutase (SOD) detection – one of the primary antioxidant enzymes: increased MnSOD protects normal tissue against oxidative stress. MnSOD as one of the SOD enzymes is a critical antioxidant enzyme residing in mitochondria. The isolated organs (intestine and hepatopancreas) were fixed in Karnovsky fixative (2h, 4 °C) and then permeabilized in PBS/0.1% v/v Triton X-100 pH 7.4 for 5 min at room temperature. In addition, tissues were blocked in PBS/5% w/v BSA pH 7.4 for 20 min and stained with primary antibody: anti-MnSOD rabbit polyclonal antibody (1:500; Stressgen) overnight at room temperature. Tissues were washed with PBS (pH 7.4) and incubated with goat anti-rabbit IgG secondary antibody conjugated with Alexa Fluor 488 (1:1000, Invitrogen). After washing the material with PBS, it was labeled with DAPI (30 min in darkness). The slides were analyzed with an Olympus FluoView FV1000 confocal microscope.

Sample preparation for Western blot analysis

Individuals of *N. davidi* from the control group were slightly anesthetized on ice and midguts were dissected (5 per sample). The midguts were then homogenized on ice in TBS buffer (Tris-buffered saline). Homogenates were then centrifuged at 4 °C, 15 000 *g* for 10 min. In the supernatants, total protein concentration was measured (*Bradford, 1976*) and detection of superoxide dismutase (MnSOD) was performed.

Western blot analysis

Denatured samples (water bath, 5 min, 95°C) of identical amounts of protein (25 µg) were loaded and separated by 10% SDS-PAGE (30 min at 90 V, then 1 h at 120 V) and then transferred to the nitrocellulose membrane (Optitran BA-S 85,Whatman) with Mini Transfer-

Blot (BIO-RAD) (2 h at 150 V, 300 mA). Next, the membranes were blocked (3% bovine serum albumin (BSA) in Tris-buffered saline (TBS), 1 h, at room temperature (RT)). Blots were incubated with specific primary antibody: anti-superoxide dismutase (MnSOD) developed in rabbit (Sigma) (overnight, at 4 °C, with continuous shaking). After incubation, the membranes were washed four times for 5 min in TBS with 0.1% Tween-20 (TBST) and then incubated with secondary antibody: Goat anti-rabbit IgG, AP conjugate (Enzo Life Sciences) (1h, at RT, continuously shaking). Dilutions of the antibodies were conducted following the manufacturer's instructions, in 1% BSA in TBS. After washing (4 x 5 min in TBST), the antibody complex was visualized by BCIP/NBT Solution (BioShop), washed again in distilled water, dried, and scanned.

Total protein concentration

Total protein concentration was measured according to the Bradford method (1976). The method is based on the binding of aromatic amino acids to the Coomassie Brilliant Blue (CBB, G-250, Sigma) dye with the v/v 1 (sample): 50 (CBB solution) ratio. The absorbance was measured at the wavelength of 595 nm, and the color intensity is proportional to protein concentration. The protein concentration was calculated from the calibration curve prepared from the absorbance measurements of the bovine serum albumin (protein content > 95%, Sigma) solutions of known concentrations (*Bradford, 1976*).

Flow cytometry

The dissected organs isolated from specimens from each experimental group were mechanically fragmented with scissors and suspended in 100 µL of PBS (pH 7.4). Then, the intestine and

hepatopancreas cells were separated by gentle shaking in a homogenizer (Minilys, Bertin Technologies). The cell suspension was washed using centrifugation at 1500 rpm for five minutes and the precipitate was suspended in 100 μL of PBS buffer.

For the quantitative measurements of cellular populations undergoing oxidative stress were used the Muse Oxidative Stress Kit (Merck Millipore, № MCH100111). The assay is based on dihydroethidium (DHE), which upon reaction with superoxide anions undergoes oxidation, resulting in red fluorescence. According to the manufacturer's protocol, the results were expressed as the percentage of two populations of cells: ROS negative (live cells) and ROS positive (cells exhibiting ROS). The measurements were performed using the Beckman Coulter Instrument FC 500 flow cytometer with a 488 nm argon laser.

Statistical analysis

Statistical analyses were performed using the STATISTICA 10.0 software package (StatSoft, Inc. (2010) version 10.0. http://www.statsoft.com). Normality was checked using the Shapiro-Wilk test. The data were tested for homogeneity of variance using Levene's test of equality of error variances. The significance of the differences in the percentage of ROS positivity between organs within the complementary groups was assessed using Student's t-test, $p<0.05$. The significance of differences in the percentage of ROS positivity among different time periods of starvation and re-feeding after starvation within each organ was assessed using the Tukey test, $p<0.05$. All assays were based on 5-6 samples, performed in duplicate.

Results

Our previous studies have shown that there are no differences in the structure and changes in the intestinal epithelium of females and males (*Włodarczyk et al., 2017, 2018*). Therefore, these studies represent the results with the omission of *N. davidi* sexes. The use of dihydroethidine (DHE) for *N. davidi* intestine and hepatopancreas revealed a diverse distribution of ROS in all experimental groups. A weak signal was seen in some of the cells in both organs in the control group (Figs. 1A-B). The quantitative analysis showed 2.8%±1.2 and 1.3%±0.6 ROS-positive cells in the hepatopancreas and intestine respectively (Table 2). After 14 days of starvation the percentage of ROS-positive cells strongly increased: 13.2%±2.1 in the hepatopancreas and 12.7%±1.2 in the intestine (Table 2). The qualitative analysis confirmed this, showing strong signals in both organs examined (Figs. 1C-D). Re-feeding for 4 days after 14 days of starvation caused an increase in the number of ROS-positive cells in the hepatopancreas 15.7%±4.4, while in the intestine their number decreased to (9.2%±4.3) in comparison to animals starved for 14 days (Table 2). The signals from hepatopancreatic cells were stronger, whereas signals from intestinal cells were weaker according to the previous experimental group (Figs. 1E-F). However, 7 days of re-feeding after starvation caused a strong decrease in the number of ROS-positive cells in both organs analyzed – 5.4%±1.8 (hepatopancreas) and 2.0%±0.4 (intestine) (Table 2) – which was confirmed by the weak signals from epithelial cells in both organs (Figs. 1G-H). Epithelial cells in hepatopancreas and intestine isolated from animals starved for 14 days and re-fed for 14 days also emitted weak signals (Figs. 2A-B). The quantitative analysis showed that the number of ROS-positive cells in the hepatopancreas decreased in comparison to animals re-fed for 7 days (4.2%±0.6), while it was the same in the intestine: 2.0%±0.4 (Fig. 3) (Table 2).

The immunofluorescent method for detecting superoxide dismutase (MnSOD) at the level of the light microscope revealed a low level of this enzyme in the intestinal and hepatopancreatic

cells in the control specimens of *N. davidi.* The specificity of the antibodies was confirmed by Western blot technique (Fig. 4). The mitochondria of the epithelial cells in both organs in animals starved for 14 days expressed a higher amount of MnSOD in comparison to the control group. The longer the animals were re-fed after 14 days of starvation, the weaker were the signals emitted by epithelial cells in the hepatopancreas and intestine (Figs. 5A-H, 6A-B).

Discussion

In recent years, intensive studies connected with the response of organisms to the stress of starvation/fasting in invertebrates have been carried out. In the studied invertebrate species, the authors described the susceptibility to starving and changes at the ultrastructural level in the epithelium of the digestive system (*Wilczek et al., 2014; Lipovšek et al., 2015, 2018; Lipovšek and Novak, 2015; Rost-Roszkowska et al., 2018*), including crustaceans (*Cervellione et al., 2017; Pantãleo et al., 2015*; *Sacristán et al., 2014, 2016; Włodarczyk, 2017, 2019*). Ultrastructural changes may be associated with an increase in the concentration of free radicals in the examined cells (*Kaminskyy and Zhivotovsky, 2014; Chen et al., 2009; Redza-Dutordoir et al., 2016*). Free radicals could derive either from numerous essential enzymatic and nonenzymatic reactions or can be caused by external stressors such as xenobiotics, X-rays, pathogens or even periods of starvation. Hence, the animals developed numerous defense mechanisms which participate in homeostasis maintenance. One of them is the production of antioxidants such as superoxide dismutases, catalase, glutathione, thioredoxin, etc. (*Borković et al., 2008; Ighodaro and Akinloye, 2018; Mailloux, 2018*). When the balance between free radical generation and antioxidant defenses is disturbed, oxidative stress occurs (*Bagchi and Puri, 1998; Combelles et al., 2009; Ramalho-Santos et al., 2009; Lobo et al., 2010*). Antioxidant non-enzymatic and

enzymatic mechanisms are involved in the response to stressful conditions in crustaceans. Mainly two enzymes, catalase and superoxide dismutase (SOD), are treated in these aquatic invertebrates as the major indicators of oxidative stress (*Borković et al., 2008; Mohana et al., 2016, Soberanes-Yepiz et al., 2018*). The level of lipids and proteins in animals' diet has an effect on the course of antioxidative processes (*Zenteno-Savin et al. 2008, Goda, 2008, ; Sacristán et al., 2016; Méndez-Martínez et al., 2018; Soberanes-Yepiz et al., 2018*). Starved crayfish showed alterations in level of lipids, glycogen, and glutathione, but fasting did not affect the level of catalase, protein oxidation or activity of some enzymes. Long-term starvation also causes a decrease in the number of molts in crustaceans, suggesting that they do not adapt to long periods of fasting (*Sacristán et al., 2016).* The effect of diet on the activation of defense mechanisms against oxidative stress has been presented for e.g. *Macrobrachium americanum* (*Soberanes-Yepiz et al., 2018*), *M. rosembergii* (*Mohana et al., 2016*), *Penaeus monodon* (*Sivagnanavelmurugan et al., 2014*) and *Cherax quadricarinatus* (*Sacristán et al., 2016*). The transport of oxygen by copper from haemocyanin in crustaceans caused that Cu/ZnSOD has been replaced by MnSOD (*Brouwer et al.,* 2003). Additionally, in these aquatic arthropods two types of this enzyme have been described: cytMnSOD and mtMnSOD. While mtMnSOD is commonly distributed in crustaceans as in the other animals, cytMnSOD has been only found in many species of prawns, crabs, lobsters, shrimps (*Brouwer et al., 2003; Lin et al. 2010; Gomez-Anduro et al., 2006, 2012; Zhao et al., 2014; Soberanes-Yepiz et al., 2018*). Total MnSOD in crustaceans is treated not only as a defense response against fasting, but also as an important factor in the immune responses against pathogen infections (*Zhang et al., 2007, Yu et al., 2011*), metal exposure (*Haque et al., 2018*) and even water pollution and ozonization (*Oropesa et al., 2017*). The relationship between oxidative stress and total MnSOD activation as the effect of starvation

has also been described in starved specimens of *N. davidi*. Under the influence of two-week fasting, an increase in the concentration of free radicals from 2.8% and 1.3% to 13.2% and 12.7% (for the hepatopancreas and the intestine, respectively) and an increase in antioxidant (MnSOD) production were observed. In this study, the change in total MnSOD concentration was investigated, which could be an introduction to further studies. To learn about the regulation of antioxidative protection, future research on the MnSOD genes is necessary. However, one of the important stages of our experiment was the observation of antioxidative processes due to the re-feeding of animals after the period of starvation, which can lead to the death of half of the population. It should be mentioned that the period of 14 days of starvation and 4, 7, and 14 days of regeneration after returning to feeding were selected in accordance with our previous studies in which the PNR_{50} for *N. davidi* was presented (*Włodarczyk et al., 2017, 2019*). Differences in the values between the hepatopancreas and intestine during fasting are not statistically significant, so it can be concluded that the concentration of free radicals in both organs forming the midgut changes similarly. The results of our research suggest the occurrence of oxidative stress in the first stage of starvation and the activation of anti-ROS defense. In the initial stage of starvation, a rapid increase in the amount of free radicals leads to oxidative stress, which activates the defense mechanism in the form of antioxidant production as has been suggested for other crustaceans (*Brouwer et al., 2003; Lin et al. 2010; Gomez-Anduro et al., 2006, 2012; Zhao et al., 2014; Sacristán et al., 2016; Soberanes-Yepiz et al., 2018*). After reaching a high level of antioxidants, there is a gradual decrease in the concentration of free radicals caused by re-feeding. Differences in the concentration of free radicals between the hepatopancreas and the intestine after returning to feeding are statistically significant, but they are very small, which indicates that both organs react similarly. Our previous study also describes the effect of

starvation and re-feeding of *N. davidi* on changes in ultrastructure and mitochondrial membrane potentials in hepatopancreatic and intestinal epithelial cells. Mitochondria are organelles which participate not only in ATP production, but also in synthesis of ROS, antioxidative enzymes, cell death activation, etc. (*Fernandez-Checa, 2003; Faron et al., 2015; Małota et al., 2019*). Additionally, these organelles can contain up to twelve sources of $O_2\bullet-/H_2O_2$ (*Mailloux, 2018*). The first signal of changes appearing in the mitochondria is the alteration in the transmembrane mitochondrial potential (ΔCm) (*Faron et al., 2015; Sonakowska et al. 2016*). Ultrastructural alterations together with transmembrane potential (ΔCm) may be connected with the activation of cell death (*Sonakowska et al., 2016*). We reported that starvation activates the degeneration of epithelial cells in *N. davidi* at the ultrastructural level and it causes an increase of cells with depolarized (non-active) mitochondria, while after re-feeding the mitochondria were regenerated at the ultrastructural level and the number of cells with active (polarized) mitochondria increased (*Włodarczyk et al., 2017*). Comparing the results of ROS activation and mitochondria degeneration, we can state that the increase in free radicals occurs together with a decreasing number of active mitochondria. The number of mitochondria with altered membrane potential also reaches a maximum after a period of 2 weeks of fasting (*Włodarczyk et al., 2017*). After re-feeding the shrimps, a decrease in the level of free radicals was observed as well as an increase in mitochondrial activity in the hepatopancreas and intestine. This may indicate an increase in electron leakage while reducing the mitochondrial membrane potential. Thus, increasing the production of free radicals does not have to be associated with greater mitochondrial activity (*Speakman et al., 2004; Faron et al., 2015*).

Depending on the level of ROS in the cell, different processes may proceed. At a low ROS level, the cell remains in a quiescent state, not dividing, and not differentiating. The

increase in the level of ROS causes the beginning of proliferation, differentiation or even cell death. Therefore, the level of ROS in cells determines the maintenance of tissue homeostasis and repair of damaged tissues (*Zhou et al., 2014*). Research in recent years (*Karpeta-Kaczmarek et al., 2016; Dziewięcka et al., 2017*) has shown the relationship between free radicals and cell death. Free radicals are an important element of signaling pathways of cell death processes. Oxidation of various chemical compounds by ROS leads to the release of e.g. cytochrome c from mitochondria, which is a signal that triggers apoptosis (*Lobo et al., 2010; Kaminskyy and Zhivotovsky, 2014*). Excessive concentration of ROS, in turn, causes oxidation of lipids, impairing the functioning of mitochondria, and decreases in ATP concentration, consequently causing necrosis. Cell death can also be activated by the first product of deactivation of superoxide ions, i.e. hydrogen peroxide (H_2O_2). If the enzymatic protection of the cell against H_2O_2 does not work, the Fenton reaction leads to the formation of toxic hydroxyl radicals (OH), against which the cell cannot defend itself. Hydroxyl radicals oxidize lipids in the membranes of various organelles, causing DNA damage and ultimately leading to apoptosis or necrosis (*Chen et al., 2009; Redza-Dutordoir et al., 2016*). The relationship between the concentration of free radicals and cell death has been described in many organs of crustaceans (*Menze et al., 2010; Wang et al., 2013*) and it has also been presented due to an experiment that was carried out aimed at studies of the intensity of apoptosis during fasting and re-feeding (*Włodarczyk et al., 2019*). After two weeks of fasting, the intensity of apoptosis in the hepatopancreas and the intestine increases almost twofold, while after returning to feeding, regeneration takes place, so the intensity of apoptosis decreases. Two weeks after re-feeding, the intensity of apoptosis is close to zero. The excess of free radicals produced induces apoptosis, the maximum of which is for two weeks of starvation. During this time, the highest level of free radicals is also observed

348 (13.2, 12.7% for the hepatopancreas and the intestine, respectively). However, the decrease in
349 the intensity of apoptosis to the level of 0 after two weeks from the return to feeding is
350 particularly interesting (*Włodarczyk et al., 2019*). This correlates with a decrease in ROS from
351 13.2 and 12.7% to 4.2 and 2% for the hepatopancreas and intestine, respectively, two weeks after
352 re-feeding. Suspension of apoptosis after the regeneration period can be explained by the
353 excessive level of antioxidants, which show a delay in relation to changes in free radical
354 concentrations. The correlation between a high concentration of free radicals and the intensity of
355 apoptosis is greater in the case of the intestine. In the case of the hepatopancreas, a significant
356 increase in the amount of free radicals induces apoptosis to a lesser extent. It can be assumed that
357 the hepatopancreas is the organ that has developed better defenses against free radicals (*Borković*
358 *et al., 2008; Goda, 200; Méndez-Martínez et al., 2018; Soberanes-Yepiz et al., 2018*). However,
359 in crustaceans total SOD activities were lower in this organ in comparison to gills and muscle
360 *(Borković et al., 2008*).

361 Oxidative stress, and therefore the imbalance between ROS and antioxidants, has serious
362 consequences for organisms. Free radicals as highly reactive compounds can cause DNA
363 mutations and damage to genes responsible for the production of antioxidant proteins (*Bagchi*
364 *and Puri, 1998 Hensley et al., 2000; Golden et al., 2002; Faron et al., 2015*). As a result, cells
365 that are subjected to long-term oxidative stress can lose their defense against free radicals over
366 time, by impairing the production of antioxidants. Superoxide dismutases (SODs) are enzymes
367 which are responsible for the breakdown of the superoxide anion into oxygen and hydrogen
368 peroxide.

369 It has been shown that starving shrimps causes a significant increase in the level of free radicals
370 and a subsequent defense response in the form of an increase in the amount of antioxidants –

here MnSOD. This means that the cells are subjected to strong oxidative stress, especially through the initial fasting period. The fasting can thus affect the impairment of the defense system against free radicals, and thus have adverse long-term effects. Regeneration after feeding starved shrimp can therefore be apparent because it does not take into account the irreversible changes that could have occurred in the cell's DNA.

Conclusions

Studies on *N. davidi* shrimp have shown that: (a) long-term starvation increases the concentration of free radicals and MnSOD concentration in the intestine and hepatopancreas; (b) return to feeding causes a decrease in free radicals and in the concentration of MnSOD in the intestine and hepatopancreatic; (c) a distinct relationship between MnSOD concentration, ROS activation, cell death activation and changes in the mitochondrial membrane potential can be observed.

References

Bagchi K, Puri S. 1998. Free radicals and antioxidants in health and disease. *East Mediterranean Health Journal* 4(2):350-360.

Banniste J, Bannister W, Rotilio G. 1987. Aspects of the structure, function, and applications of superoxide dismutase. *Critical Reviews in Biochemistry* 22:111–80

Borković SS, Pavlović SZ, Kovacević TB, Stajn AS, Petrović VM, Saicić ZS. 2008. Antioxidant defence enzyme activities in hepatopancreas, gills and muscle of Spiny cheek crayfish (*Orconectes limosus*) from the River Danube. *Comparative Biochemistry and Physiology - Part C Toxicology and Pharmacology* 147(1):122-8

393 Bradford MM. 1976. A rapid and sensitive method for the quantitation of microgram quantities
394 of protein utilizing the principle of protein-dye binding. *Analitical Biochemistry* 72:248–254
395 Brouwer M, Hoexum BT, Grater W, Brown-Peterson N. 2003. Replacement of a cytosolic
396 copper/zinc superoxide dismutase by a novel cytosolic manganese superoxide dismutase in
397 crustaceans that use copper (haemocyanin) for oxygen transport. *Biochemical Journal* 374:219-
398 228
399 Cadenas E, Davies KJA. 2000. Mitochondrial free radical generation, oxidative stress, and aging.
400 *Free Radical Biology and Medicine* 29(3–4):222-230
401 Cao X, Antonyuk SV, Seetharaman SV, Whitson LJ, Taylor AB, Holloway SP, Strange RW,
402 Doucette PA, Valentine JS, Tiwari A, Hayward LJ, Padua S, Cohlberg JA, Hasnain SS, Hart PJ.
403 2008. Structures of the G85R variant of SOD1 in familial amyotrophic lateral sclerosis. *The*
404 *Journal of Biological Chemistry* 283:16169–77
405 Cervellione F, McGurk C, Van Den Broeck W. 2017. Effect of starvation and refeeding on the
406 ultrastructure of the perigastric organ (hepatopancreas) in the whiteleg shrimp *Litopenaeus*
407 *vannamei* (Boone, 1931) (Decapoda: Caridea: Penaeidae). *Journal of Crustacean Biology*
408 37(6):693-700
409 Chen Y, Azad MB, Gibson SB. 2009. Superoxide is the major reactive oxygen species regulating
410 autophagy. *Cell Death & Differentiation* 16(7):1040–1052
411 Combelles CMH, Gupta S. 2009. Could oxidative stress influence the in-vitro maturation of
412 oocytes? *Reproductive BioMedicine Online* 18(6):864-880
413 Dziewięcka M, Karpeta-Kaczmarek J, Augustyniak M, Rost-Roszkowska M. 2017. Short-term *in*
414 *vivo* exposure to graphene oxide can cause damage to the gut and testis. *Journal of Hazardous*
415 *Materials* 328:80-89

416 Faron J, Bernaś T, Sas–Nowosielska H, Klag J. 2015. Analysis of the Behavior of Mitochondria
417 in the Ovaries of the Earthworm *Dendrobaena veneta* Rosa. *PLoS ONE* 10(2):0117187
418 Fernández-Checa JC. 2003. Redox regulation and signaling lipids in mitochondrial apoptosis.
419 *BRC Biochemical and Biophysical Research Communications* 304(3):471-479
420 Fridovich I. 1995. Superoxide radical and superoxide dismutases. *Annual Review of*
421 *Biochemistry* 64:97-112
422 Goda AMAS. 2008. Effect of dietary protein and lipid levels and protein-energy ratio on growth
423 indices feed utilization and body composition of freshwater prawn, *Macrobrachium rosenbergii*
424 (de Man, 1879) postlar-vae. *Aquaculture Research* 39:891-901
425 Golden TR, Hinerfeld DA, Melov S. 2002. Oxidative stress and aging: beyond correlation. *Aging*
426 *Cell* 1(2):117-123
427 Gómez-Anduro GA, Ascencio-Valle F, Peregrino-Uriarte AB, Cámpa-Córdova A, Yepiz-
428 Plascencia G. 2012. Cytosolic manganese superoxide dismutase genes from the white shrimp
429 *Litopenaeus vannamei* are differentially expressed in response to lipopolysaccharides, white spot
430 virus and during ontogeny. *Comparative Biochemistry and Physiology, Part B*, 162(4):120-5
431 Haque MN, Lee DH, Kim BM, Nam SE, Rhee JS. 2018. Dose- and age-specific antioxidant
432 responses of the mysid crustacean *Neomysis awatschensis* to metal exposure. *Aquatic Toxicology*
433 201:21-30
434 Hensley K, Robinson KA, Gabbita SP, Salsman S, Floyd RA. 2000. Reactive oxygen species cell
435 signaling and cell injury. *Free Radical Biolology & Medicine* 28(10):1456–1462
436 Herrera‐Álvarez L, Fernández I, Benito J, F. 2000. Ultrastructure of the midgut and hindgut of
437 *Derocheilocaris remanei* (Crustacea, Mystacocarida). *Journal of Morphology* 244:177-189
438 Kaminskyy VO and Zhivotovsky B. 2014. Free radicals in cross talk between autophagy and
439 apoptosis. *Antioxidants & Redox Signaling* 21(1):86–102

Kamogashira T, Fujimoto C, Yamaosba T. 2015. Reactive oxygen species, apoptosis, and mitochondrial dysfunction in hearing loss. BioMed Research International 2015:1-7

Karpeta-Kaczmarek J, Dziewięcka M, Augustyniak M, Rost-Roszkowska M, Pawlyta M. 2016. Oxidative stress and genotoxic effects of diamond nanoparticles. *Environmental Research* 148:264-272

Lin YC, Lee FF, Wu CL, Chen JC. 2010. Molecular cloning and characterization of a cytosolic manganese superoxide dismutase (cytMnSOD) and mitochondrial manganese superoxide dismutase (mtMnSOD) from the kuruma shrimp *Marsupenaeus japonicus*. Fish and Shellfish Immunology 28:143–150

Lipovšek S, Novak T. 2015. Autophagy in the fat body cells of the cave cricket *Troglophilus neglectus* Krauss, 1878 (Rhaphidophoridae, Saltatoria) during overwintering. *Protoplasma* 253(2):457-66

Lipovšek S, Novak T, Janžekovič F, Leitinger G. 2015. Changes in the midgut diverticula in the harvestmen *Amilenus aurantiacus* (Phalangiidae, Opiliones) during winter diapause. *Arthropod Structure and Development* 44(2):131-41

Lipovšek S, Leitinger G, Novak T, Janžekovič F, Gorgoń S, Kamińska K, Rost-Roszkowska M. 2018. Changes in the midgut cells in the European cave spider, *Meta menardi*, during starvation in spring and autumn. *Histochemistry and Cell Biology* 149(93):245–260

Lobo V, Patil A, Phatak A, Chandra N. 2010. Free radicals, antioxidants and functional foods: Impact on human health. *Pharmacognosy Reviews* 4(8):118–126

Mailloux RJ. 2018. Mitochondrial antioxidants and the maintenance of cellular hydrogen reroxide levels. *Oxidative Medicine and Cellular Longevity* https://doi.org/10.1155/2018/7857251

463 Malota K, Student S, Świątek P. 2019. Low mitochondrial activity within developing earthworm
464 male germ-line cysts revealed by JC-1. *Mitochondrion*
465 https://doi.org/10.1016/j.mito.2018.01.007
466 Martin LJ. 2010. Mitochondrial and Cell Death Mechanisms in Neurodegenerative Diseases.
467 *Pharmaceuticals*3:839–915
468 Méndez-Martínez Y, García-Guerrero MU, Arcos-Ortega FG, Martínez-Córdova LR,
469 Yamasaki-Granados S, Pérez-Rodríguez JC, Cortés-Jacinto E. 2018b. Effect of different ratios of
470 dietary protein-energy on growth, body proximal composition, digestive enzyme activity, and
471 hepatopancreas histology in *Macrobrachium americanum* (Bate, 1868) prawn juveniles.
472 *Aquaculture* 485: 1-11.
473 Menze MA, Fortner G, Nag S, Hand S.C. 2010. Mechanisms of apoptosis in Crustacea: what
474 conditions induce versus suppress cell death? *Apoptosis* 15:293–312
475 Mohana K, Padmanaban AM, Uthayakumara V, Chandirasekar R, Muralisankar T, Santhanam
476 R. 2016. Effect of dietary *Ganoderma lucidum* polysaccharides on biological and physiological
477 responses of the giant freshwater prawn *Macrobrachium rosenbergii*. *Aquaculture* 464: 42-49
478 Oropesa AL, Floro AM, Palma P. 2017. Toxic potential of the emerging contaminant nicotine to
479 the aquatic ecosystem. *Environmental Science and Pollution Research* 24(20):16605-16616
480 Pantaleão JAF, Barros-Alves S, Tropea C, Alves DFR, Negreiros-Fransozo ML, López-Greco
481 LS. 2015. Nutritional vulnerability in early stages of the freshwater ornamental "red cherry
482 shrimp" *Neocaridina davidi* (Bouvier, 1904) (Caridea: Atyidae). *Journal of Crustacean Biology*
483 35(5):676–681

Ramalho-Santos J, Varum S, Sandra Amaral, MotaPC, Sousa AP, Amaral A. 2009. Mitochondrial functionality in reproduction: from gonads and gametes to embryos and embryonic stem cells. *Human Reproduction Update* 15(5):553–572

Ratcliffe NA, King PE. 1969. Morphological, ultrastructural, histochemical and electrophoretic studies on the venom system of *Nasonia vitripennis* walker (hymenoptera: Pteromalidae). *Journal of Morphology* 127:177–203

Redza-Dutordoir M, Averill-Bates DA. 2016. Activation of apoptosis signalling pathways by reactive oxygen species Maureen. *Biochimica et Biophysica Acta (BBA) - Molecular Cell Research* 1863(12):2977-2992

Rost-Roszkowska MM, Janelt K, Poprawa I. 2018. The role of autophagy in the midgut epithelium of Parachela (Tardigrada). *Zoomorphology* 137(4):501–509

Sacristán HJ, Nolasco-Soria H, López Greco LS. 2014. Effect of attractant stimuli, starvation period, and food availability on digestive enzymes in the redclaw crayfish *Cherax quadricarinatus* (Parastacidae). *Aquatic Biology* 23:87–99

Sacristán HJ, Ansaldo M, Franco-Tadic LM, Fernández Gimenez AV, López Greco LS. 2016. Long-term starvation and posterior feeding effects on biochemical and physiological responses of midgut gland of *Cherax quadricarinatus* juveniles (Parastacidae). *PLoS ONE* 11(3): e0150854

Soberanes-Yepiz ML, Méndez-Martínez Y, García-Guerrero MU, Ascencio F, Violante-González J, García-Ibañez S, Cortés-Jacinto E. 2018. Superoxide dismutase activity in tissues of juvenile cauque river prawn (*Macrobrachium americanum* Bate, 1868) fed with different levels of protein and lipid. *Latin American Journal of Aquatic Research* 46(3):543-555

505 Sonakowska L, Włodarczyk A, Wilczek G, Wilczek P, Student S, Rost-Roszkowska MM. 2016.
506 Cell death in the epithelia of the intestine and hepatopancreas in *Neocaridina heteropoda*
507 (Crustacea, Malacostraca). *PLos ONE* 11(2):0147582
508 Sonakowska L, Włodarczyk A, Poprawa I, Binkowski M, Śróbka J, Kamińska K, Kszuk-
509 Jendrysik M, Chajec Ł, Zajusz B, Maria Rost-Roszkowska M. 2015. Structure and ultrastructure
510 of the endodermal region of the alimentary tract in the freshwater shrimp *Neocaridina*
511 *heteropoda* (Crustacea, Malacostraca). *PLoS ONE* 10(5):0126900
512 Sousa L, Petriella AM. 2006. Morphology and histology of *P. argentinus* (Crustacea,
513 Decapoda,Caridea) digestive tract. *BIOCELL* 30(2):287-294
514 Speakman JR, Talbot DA, Selman C, Snart S, McLaren JS, Redman P, Krol E, Jackson DM,
515 Johnson MS, Brand MD. 2004. Uncoupled and surviving: Individual mice with high metabolism
516 have greater mitochondrial uncoupling and live longer. *Aging Cell* 3:87-95
517 Umasuthan N, Bathige SD, Revathy KS, Lee Y, Whang I, Choi CY, Park HC, Lee J. 2012. A
518 manganese superoxide dismutase (MnSOD) from *Ruditapes philippinarum*: comparative
519 structural- and expressional-analysis with copper/zinc superoxide dismutase (Cu/ZnSOD) and
520 biochemical analysis of its antioxidant activities. *Fish and Shellfish Immunology* 33(4):753-65.
521 Wang J, Zhang P, Shen Q, Wang Q, Liu D, Li J Wang, L. 2013. The effects of cadmium
522 exposure on the oxidative state and cell death in the gill of freshwater crab *Sinopotamon*
523 *henanense*. *PLoS One* 8, e64020
524 Wilczek G,Rost-Roszkowska M.Wilczek P, A.Babczyńska A, ,E.Szulińska E, L.Sonakowska L,
525 Marek-Swędzioł M. 2014. Apoptotic and necrotic changes in the midgut glands of the wolf
526 spider Xerolycosa nemoralis (Lycosidae) in response to starvation and dimethoate exposure.
527 *Ecotoxicology and Environmental Safety* 101:157-167

528 Włodarczyk A, Sonakowska L, Kamińska K, Marchewka A, Wilczek G, Wilczek P, Student S,
529 Rost-Roszkowska M. 2017. The effect of starvation and re-feeding on mitochondrial potential in
530 the midgut of *Neocaridina davidi* (Crustacea, Malacostraca). PLoS ONE 12(3):0173563
531 Włodarczyk A, Student S, Rost-Roszkowska MM, 2019. Autophagy and apoptosis in starved and
532 re-fed *Neocaridina davidi* (Crustacea, Malacostraca) midgut. *Canadian Journal of Zoology*
533 97(4): 294-303
534 Yao CL, Wang AL, Wang WN, SUN RY. 2004. Purification and partial characterization of Mn
535 superoxide dismutase from muscle tissue of the shrimp *Macrobrachium nipponense*.
536 *Aquaculture* 241:621-631.
537 Yao CL, Wang AL, Wang ZY, Wang WN, Sun RY. 2007. Purification and partial
538 characterization of Cu,Zn superoxide dismutase from haemolymph of oriental river shrimp,
539 *Macrobrachium nipponense*. *Aquaculture* 270:559– 565.
540 Yu Z, He X, Fu D and Zhang Y. 2011. Two superoxide dismutase (SOD) with different
541 subcellular localizations involved in innate immunity in *Crassostrea hongkongensis*. *Fish and*
542 *Shellfish Immunology* 31:533-539
543 Zelko IN, Mariani TJ, Folz RJ. 2002. Superoxide dismutase multigene family: a comparison of
544 the CuZn-SOD (SOD1), Mn-SOD (SOD2), and EC-SOD (SOD3) gene structures, evolution, and
545 expression. *Free Radical Biology and Medicine* 33(3):337-49
546 Zhang QL, Li FH, Wanf B, Zhang JQ, Liu YC, Zhou Q, Xiang JH. 2007. The mitochondrial
547 manganese superoxide dismutase gene in Chinese shrimp *Fenneropenaeus chinensis*: Cloning,
548 distribution and expression. *Developmental and Comparative Immunology* 31:429-440

549 Zhao DX, Chen LQ, Qin JG, Qin CJ, Zhang H, Wu P, Li EC. 2014. Molecular characterization
550 of a cytosolic manganese superoxide dismutase from the Chinese mitten crab, *Eriocheir sinensis*.
551 *Genetics and Molecular Research* 13(4):9429-9442.
552 Zhou D, Shao L, Spitz DR. 2014. Reactive oxygen species in normal and tumor stem cells.
553 *Advances in Cancer Research* 122:1–67.

Table legends

Table 1. Number of adult specimens of *N. davidi* used in the each part of the experiment.

Table 2. Mean (x) ± standard deviation (SD) of cells with signs of DHE in the entire intestine and proximal zone of hepatopancreatic epithelium in *N. davidi.* The different letters (a, b) denote significant differences between organs within the complementary groups (Student t-test, $p<0.05$; n = 5).

Figure legend

Figure 1. 3D representation of the DHE staining and DAPI staining of hepatopancreas and intestine. ROS-positive cells (red), nuclei (n, blue). Confocal microscope. (A) a fragment of the hepatopancreas in non-starved animals. Scale bar = 20 μM. (B) a fragment of the intestine in non-starved animals. Scale bar = 20 μM. (C) a fragment of the hepatopancreas in animals starved for 14 days. Scale bar = 20 μM. (D) a fragment of the intestine in animals starved for 14 days. Scale bar = 30 μM. (E) hepatopancreas in animals re-fed for 4 days after 14 days of starvation. Scale bar = 20 μM. (F) intestine in animals re-fed for 4 days after 14 days of starvation. Scale bar = 20 μM. (G) hepatopancreas in animals re-fed for 7 days after 14 days of starvation. Scale bar = 20 μM. (H) intestine in animals re-fed for 7 days after 14 days of starvation. Scale bar = 20 μM.

Figure 2. 3D representation of the DHE and DAPI staining of hepatopancreas and intestine. ROS-positive cells (red), nuclei (n, blue). Confocal microscope. (A) hepatopancreas in animals re-fed for 14 days after 14 days of starvation. Scale bar = 20 μM. (B) intestine in animals re-fed for 14 days after 14 days of starvation. Scale bar = 20 μM.

577 **Figure 3.** Diagrammatic representation of the average percentage of ROS-positive cells during
578 starvation and after re-feeding. Flow cytometry.

579 **Figure 4.** Western blot analysis of Superoxide Dismutase (MnSOD) in the midgut of freshwater
580 shrimp *Neocaridina davidi* (25 μg of protein per each line).

581 **Figure 5.** 3D representation of the MnSOD localization (green) and DAPI staining of
582 hepatopancreas and intestine. Nuclei (n, blue). Confocal microscope.
583 (A) a fragment of the hepatopancreas in non-starved animals. Scale bar = 30 μM. (B) a fragment
584 of the intestine in non-starved animals. Scale bar = 20 μM. (C) a fragment of the hepatopancreas
585 in animals starved for 14 days. Scale bar = 30 μM . (D) a fragment of the intestine in animals
586 starved for 14 days. Scale bar = 30 μM. (E) hepatopancreas in animals re-fed for 4 days after 14
587 days of starvation. Scale bar = 30 μM. (F) intestine in animals re-fed for 4 days after 14 days of
588 starvation. Scale bar = 20 μM. (G) hepatopancreas in animals re-fed for 7 days after 14 days of
589 starvation. Scale bar = 30 μM. (H) intestine in animals re-fed for 7 days after 14 days of
590 starvation. Scale bar = 30 μM.

591 **Figure 6.** 3D representation of the MnSOD localization (green) and DAPI staining of
592 hepatopancreas and intestine. Nuclei (n, blue). Confocal microscope.
593 (A) hepatopancreas in animals re-fed for 14 days after 14 days of starvation. Scale bar = 30 μM.
594 (B) **i**ntestine in animals re-fed for 14 days after 14 days of starvation. Scale bar = 20 μM.
595

Table 1(on next page)

Number of adult specimens of *N. davidi* used in the each part of the experiment.

Number of days of starvation	**Number of specimens analyzed Part 1: starvation**		
	Flow cytometry-DHE	**Confocal microscopy**	
		MnSOD	**DHE**
control	24	4	4
14 days	24	4	4
Number of days of re-feeding after 14 days of starvation	**Number of specimens analyzed Part 2: re-feeding after 14 days of starvation**		
	Flow cytometry-DHE	**Confocal microscopy**	
		MnSOD	**DHE**
4 days	24	4	4
7 days	24	4	4
14 days	24	4	4

Table 1. Number of adult specimens of *N. davidi* used in each part of the experiment.

Table 2(on next page)

Mean (x) ± standard deviation (SD) of cells with signs of DHE in the entire intestine and proximal zone of hepatopancreatic epithelium in *N. davidi.*

The different letters (a, b) denote significant differences between organs within the complementary groups (Student t-test, $p<0.05$; n = 5).

	Hepatopancreas	intestine
control group	2.8±1.2a	1.3±0.6a
14 days of starvation	13.2±2.1a	12.7±1.2a
4 days of re-feeding after 14 days of starvation	15.7±4.4a	9.2±4.3a
7 days of re-feeding after 14 days of starvation	5.4±1.8b	2.0±0.4a
14 days of re-feeding after 14 days of starvation	4.2±0.6b	2.0±0.4a

Table 2. Mean (x) ± standard deviation (SD) of cells with signs of DHE in the entire intestine and proximal zone of hepatopancreatic epithelium in *N. davidi.* The different letters (a, b) denote significant differences between organs within the complementary groups (Student t-test, $p<0.05$; n = 5).

Figure 1

3D representation of the DHE staining and DAPI staining of hepatopancreas and intestine. ROS-positive cells (red), nuclei (n, blue). Confocal microscope.

ROS-positive cells (red), nuclei (n, blue). Confocal microscope. (A) a fragment of the hepatopancreas in non-starved animals. Scale bar = 20 µM. (B) a fragment of the intestine in non-starved animals. Scale bar = 20 µM. (C) a fragment of the hepatopancreas in animals starved for 14 days. Scale bar = 20 µM. (D) a fragment of the intestine in animals starved for 14 days. Scale bar = 30 µM. (E) hepatopancreas in animals re-fed for 4 days after 14 days of starvation. Scale bar = 20 µM. (F) intestine in animals re-fed for 4 days after 14 days of starvation. Scale bar = 20 µM. (G) hepatopancreas in animals re-fed for 7 days after 14 days of starvation. Scale bar = 20 µM. (H) intestine in animals re-fed for 7 days after 14 days of starvation. Scale bar = 20 µM.

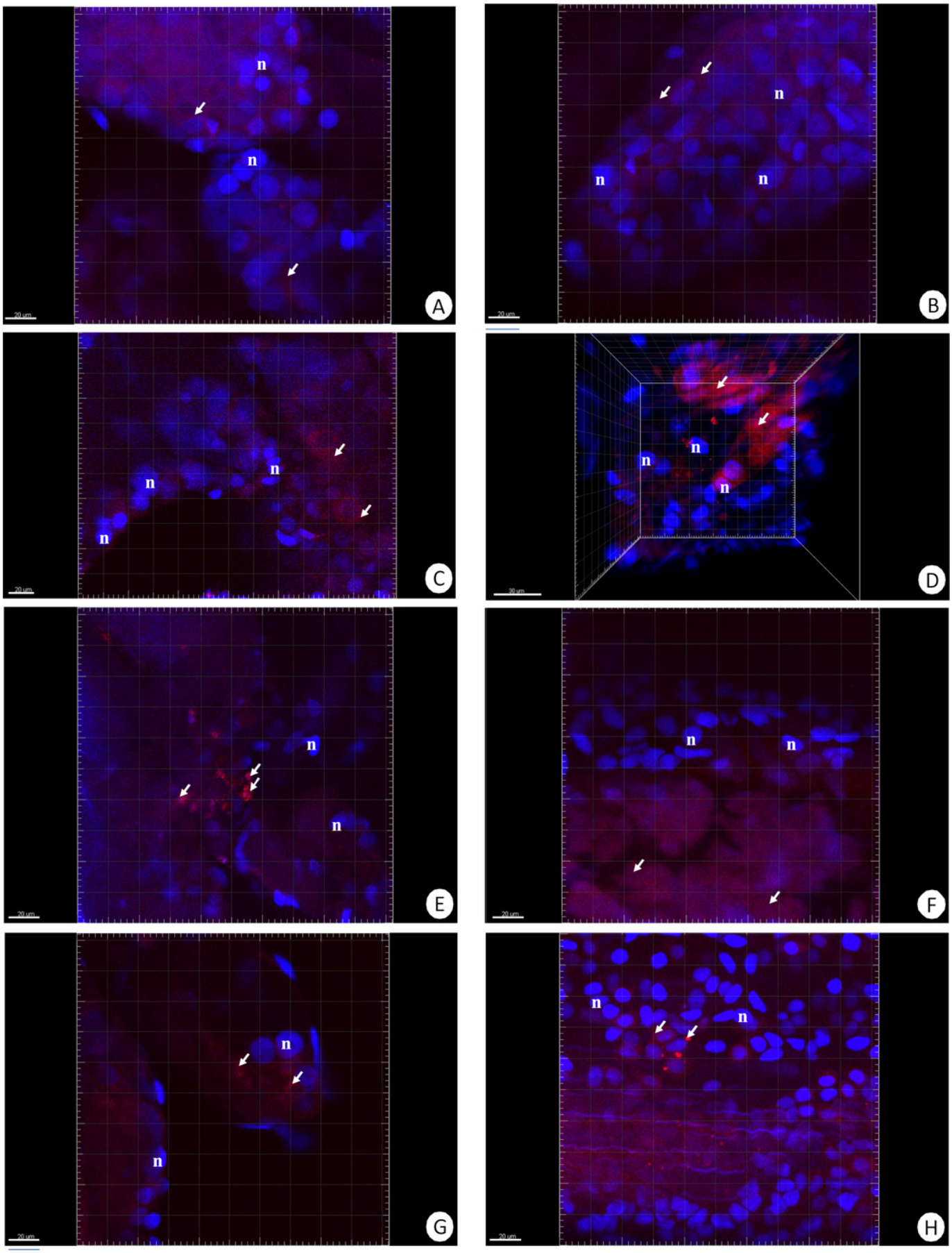
A
B
C
D
E
F
G
H

Figure 2

3D representation of the DHE and DAPI staining of hepatopancreas and intestine. ROS-positive cells (red), nuclei (n, blue). Confocal microscope.

(A) hepatopancreas in animals re-fed for 14 days after 14 days of starvation. Scale bar = 20 µM. (B) intestine in animals re-fed for 14 days after 14 days of starvation. Scale bar = 20 µM.

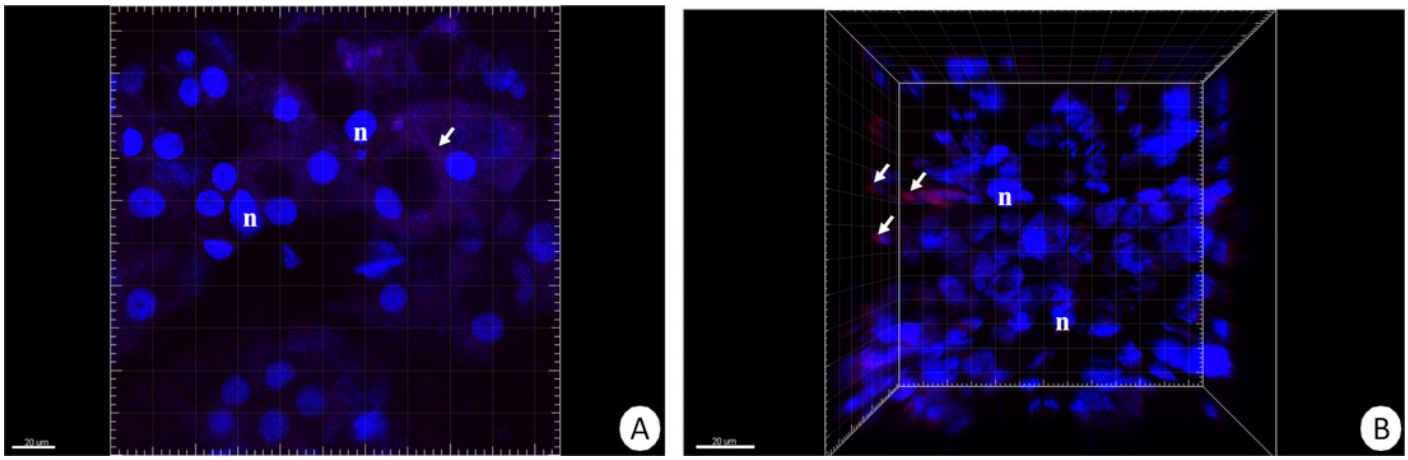

Figure 3

Diagrammatic representation of the average percentage of ROS-positive cells during starvation and after re-feeding . Flow cytometry.

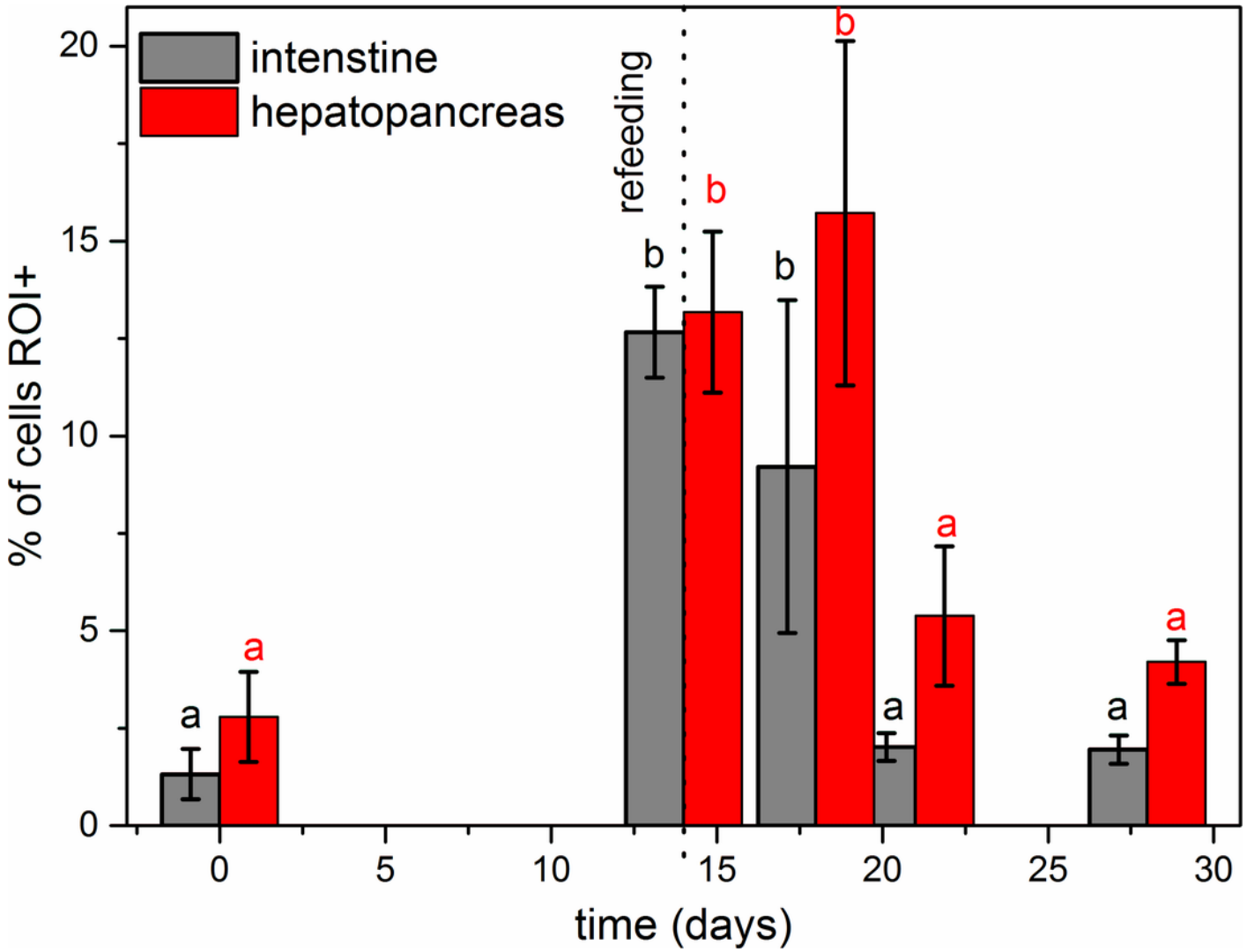

Figure 4

Western blot analysis of Superoxide Dismutase (MnSOD) in the midgut of freshwater shrimp *Neocaridina davidi* (25 μg of protein per each line).

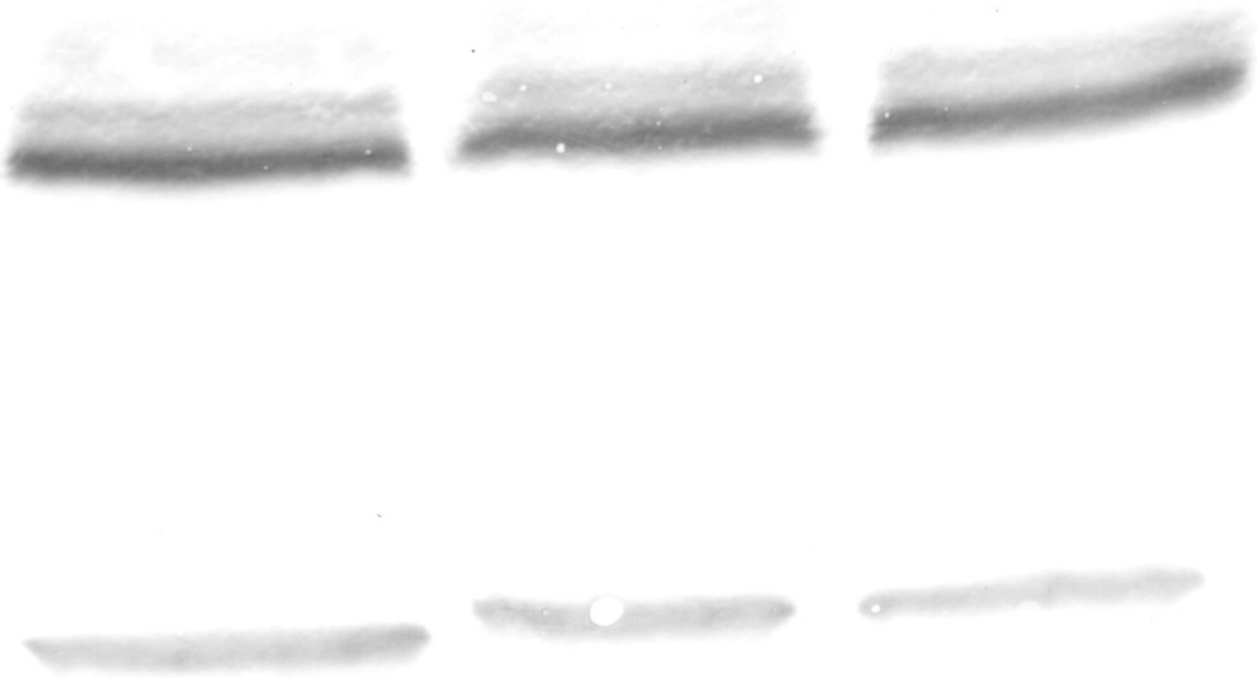

Figure 5

3D representation of the MnSOD localization (green) and DAPI staining of hepatopancreas and intestine. Nuclei (n, blue). Confocal microscope.

(A) a fragment of the hepatopancreas in non-starved animals. Scale bar = 30 µM. (B) a fragment of the intestine in non-starved animals. Scale bar = 20 µM. (C) a fragment of the hepatopancreas in animals starved for 14 days. Scale bar = 30 µM . (D) a fragment of the intestine in animals starved for 14 days. Scale bar = 30 µM. (E) hepatopancreas in animals re-fed for 4 days after 14 days of starvation. Scale bar = 30 µM. (F) intestine in animals re-fed for 4 days after 14 days of starvation. Scale bar = 20 µM. (G) hepatopancreas in animals re-fed for 7 days after 14 days of starvation. Scale bar = 30 µM. (H) intestine in animals re-fed for 7 days after 14 days of starvation. Scale bar = 30 µM.

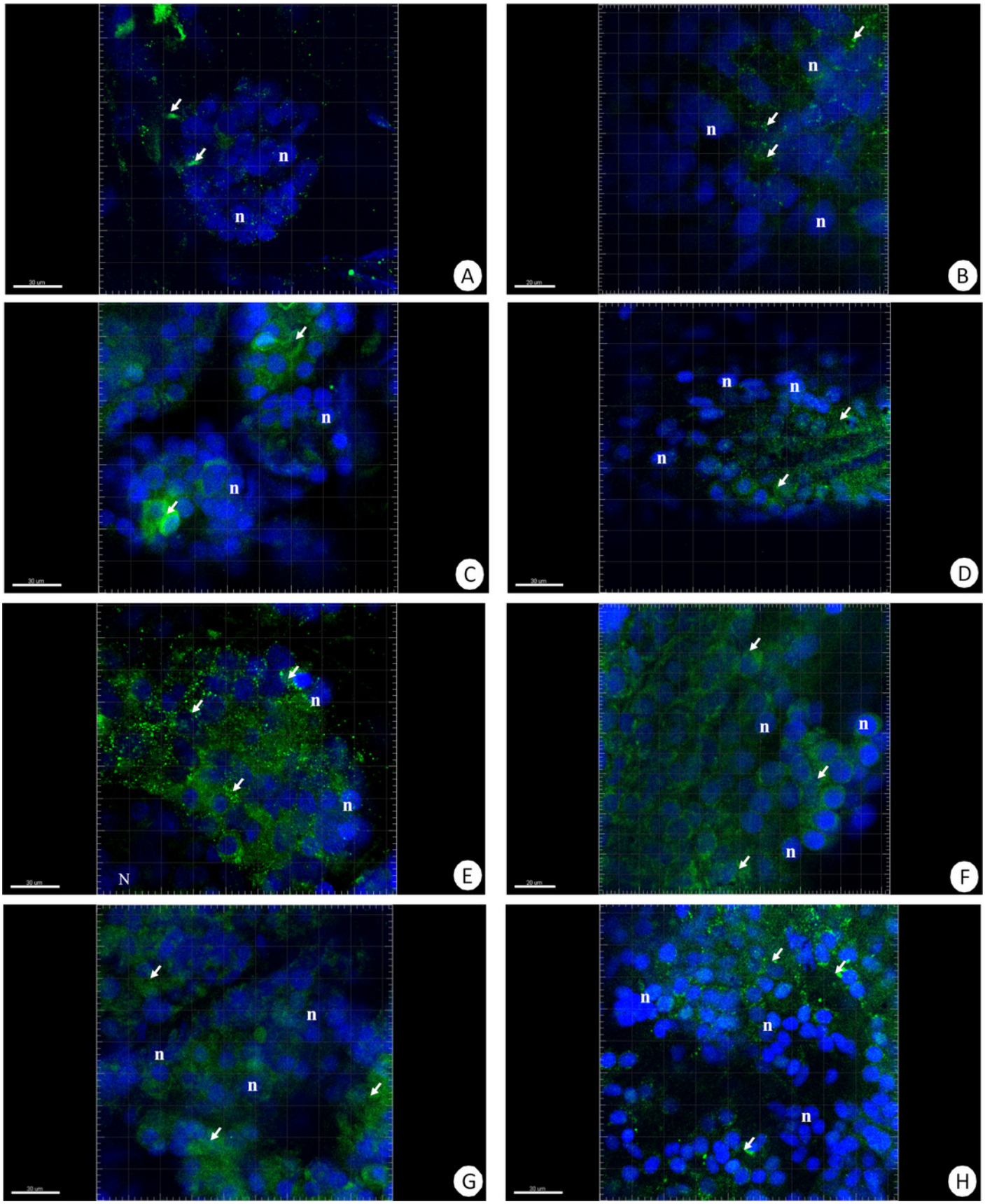
A
B
C
D
E
F
G
H
n
N

Figure 6

3D representation of the MnSOD localization (green) and DAPI staining of hepatopancreas and intestine. Nuclei (n, blue). Confocal microscope.

(A) hepatopancreas in animals re-fed for 14 days after 14 days of starvation. Scale bar = 30 µM. (B) **i**ntestine in animals re-fed for 14 days after 14 days of starvation. Scale bar = 20 µM.